Supporting Information

Exploiting Powder X-ray Diffraction to Establish the Solvent-Assisted Solid-State Supramolecular Assembly of Pillar[5]quinone

Kilingaru I. Shivakumar,[1] Yuncheng Yan,[2] Colan E. Hughes,[2] David C. Apperley,[3] Kenneth D. M. Harris,*[2] and Gangadhar J. Sanjayan*[1]

1   Division of Organic Chemistry, CSIR-National Chemical Laboratory, Dr Homi Bhabha Road, Pune 411 008, India.

2   School of Chemistry, Cardiff University, Park Place, Cardiff CF10 3AT, Wales, U.K.

3   Department of Chemistry, University of Durham, Durham DH1 3LE, U.K.

General Methods, Optical Microscopy and Electron Microscopy

Unless otherwise stated, all chemicals and reagents were obtained commercially. Optical microscopy images of *in-situ* grown P[5]Q·2TCE rods were recorded on a Nikon polarizing microscope ECLIPSE E600 POL by placing a drop of hot solution of P[5]Q in TCE on a glass slide. SEM analyses were performed on a FEI Quanta 200 3D series SEM system (dual beam ESEM) with a tungsten filament as the electron source operated at 10 kV. TEM images were recorded using a FEI Tecnai G2 F20 X-TWIN TEM at an accelerating voltage of 200 kV. *In situ* self-assembled P[5]Q·2TCE rods were grown on a carbon-coated copper grid TEM Window (TED PELLA, INC. 200 mesh) by drop-casting a hot solution of P[5]Q in TCE. Atomic Force Microscope (AFM) images of P[5]Q·2TCE were recorded using a digital instrument nanoscope-IV multimode scanning probe microscope at ambient conditions in tapping mode. Sampling was done by dispersing P[5]Q·2TCE in chloroform and drop-casting on a silicon substrate. Dispersion of P[5]Q·2TCE in chloroform was done by sonication of the solution for two minutes. Thermal analyses were performed on a PerkinElmer STA 6000 instrument. The methods used for powder X-ray diffraction and solid-state NMR spectroscopy are described below.
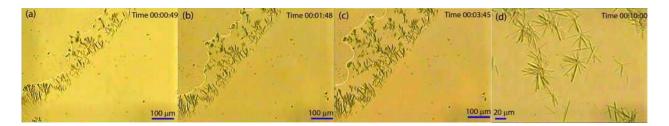

Figure S1 Optical microscopy images recorded on a time-scale showing the growth of crystals of the P[5]Q·2TCE material.
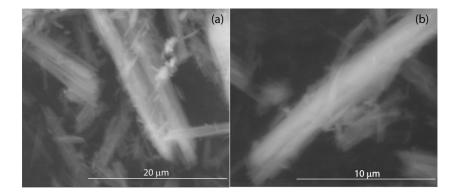

Figure S2 Representative SEM images of the material obtained following removal of the solvent TCE from the P[5]Q·2TCE material.
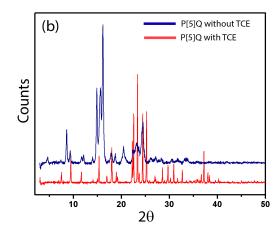
Figure S3 Experimental powder XRD patterns recorded for P[5]Q·2TCE (red) and for the material obtained by removal of the TCE component from P[5]Q·2TCE (blue).
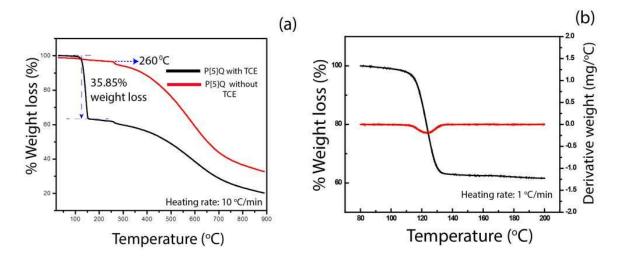

Figure S4 (a) TGA data (heating rate 10 °C/min; nitrogen atmosphere) for P[5]Q·2TCE and for the material obtained following removal of the TCE component. (b) TGA and DTG data (heating rate 1 °C/min; nitrogen atmosphere) for P[5]Q·2TCE.

Structure Determination of P[5]Q·2TCE from Powder X-ray Diffraction Data

The powder X-ray diffraction (XRD) pattern of P[5]Q·2TCE was recorded at ambient temperature in transmission mode on a Bruker D8 instrument using Ge-monochromated CuKα_1 radiation (2θ range, 4 – 50°; total time, 48 hrs).

The powder XRD pattern was indexed using the TREOR code[1] in the program CRYSFIRE,[2] giving the following unit cell with orthorhombic metric symmetry: a = 18.29 Å, b = 15.26 Å, c = 6.91 Å (V = 1929.9 Å^3). The high-resolution solid-state ^{13}C NMR spectrum indicates that there are two crystallographically distinct TCE molecules, supporting an asymmetric unit with stoichiometry P[5]Q·2TCE. Given the volume of the unit cell and consideration of density, the number of formula units P[5]Q·2TCE in the unit cell was assigned as Z = 2.

Initial profile fitting carried out using the Le Bail method[3] in the GSAS program[4] did not give an acceptable quality of fit. However, by reducing the symmetry to monoclinic and allowing one angle in the above unit cell to relax, an improved fit was achieved (R_{wp} = 1.13%; R_p = 0.87%; Figure S5) for the following unit cell: a = 18.7709(4) Å, b = 15.2498(4) Å, c = 6.90511(17) Å, β = 89.7359(15)°. The correct space group could not be assigned unambiguously on the basis of systematic absences alone and structure solution was attempted for each of the space groups P2, P2$_1$, Pm, P2$_1$/n P2/m, P2/n and P2$_1$/m. The refined unit cell and profile parameters obtained from the Le Bail fit were used in the subsequent structure-solution calculations.

Structure solution was carried out using the direct-space genetic algorithm (GA) technique[5] incorporated in the program EAGER.[6] Initially, independent GA structure-solution calculations were carried out for space groups P2, P2$_1$, Pm, P2$_1$/n P2/m, P2/n and P2$_1$/m, as discussed above. The model comprised one P[5]Q molecule and two TCE molecules for the space groups with multiplicity of 2 and one half P[5]Q molecule and one TCE molecule for the space groups with multiplicity of 4. The best fit to the experimental powder XRD data was found for space group P2$_1$. However, the model was unable to give an adequate description of one of the TCE molecules in the asymmetric unit. Indeed, the difference Fourier map contained significant features in the vicinity of this TCE molecule, suggesting the possibility that this molecule may be disordered. For this reason, a revised structural model was considered in which disorder of this TCE molecule was introduced as two distinct TCE molecules, each with occupancy of 0.5. The GA structure-solution calculation was repeated for this model in space group P2$_1$. Each trial structure was defined by a total of 26 variables (11 positional variables, 12 rotational variables and 3 torsion-angle variables). The P[5]Q molecule was treated as rigid whereas one torsion angle was varied for each TCE molecule. One positional variable (y-coordinate of the P[5]Q molecule) was fixed as the origin may be freely defined along the b-axis in space group P2$_1$.

In total, 16 independent GA structure-solution calculations were carried out. Each calculation

involved the evolution of 1000 generations for a population of 100 structures, with 10 mating operations and 50 mutation operations carried out per generation. All 16 calculations converged on essentially the same structure solution, corresponding to the lowest value of R_{wp}.

The best structure solution (i.e., the structure with lowest R_{wp} obtained in the GA calculations) was used as the initial structural model for Rietveld refinement,[7] which was carried out using the GSAS program.[4] However, refinement of the positions of the two partial-occupancy TCE molecules representing the disordered site was found to give unsatisfactory short contacts with the P[5]Q molecule. Consequently, the two TCE molecules representing the disordered site were removed from the structural model. The difference Fourier map calculated for the model with no TCE molecules in the disordered site showed two strong positions of electron deficiency and chlorine atoms were introduced into the model at each of these positions. Rietveld refinement was again performed, followed by calculation of another difference Fourier map. Again, two chlorine atoms were placed at the positions of largest electron deficiency and Rietveld refinement was performed again, followed by difference Fourier calculation. Finally, two carbon atoms were added to the structural model at the positions of highest electron deficiency and a final Rietveld refinement was carried out.

In the final Rietveld refinement, standard restraints were applied to bond lengths and bond angles and planar restraints were applied to the quinone groups. The positions of the atoms representing the disordered TCE molecule were not restrained in any way. We emphasize that the atom positions representing the disordered TCE site in this structural model represent the optimal description of the resultant "smeared-out" electron density distribution, rather than representing atom positions in a discrete TCE molecule. Separate common isotropic displacement parameters (U_{iso}) were refined for the non-hydrogen atoms of the P[5]Q molecule, the ordered TCE molecule and the disordered TCE molecule. In each case, U_{iso} for the hydrogen atoms in a given molecule was set to 1.2 times the common value for the non-hydrogen atoms in the same molecule. Refinement of preferred orientation parameters allowed the effects of a small extent of preferred orientation in the experimental data to be taken into account [March-Dollase preferential orientation plane (001); ratio, 86.5%]. The final Rietveld refinement (2θ range, 4 – 50°; 2703 profile points; 271 refined variables) gave a good fit to the powder XRD data (R_{wp} = 1.55%, R_{p} = 1.09%; Figure S6), with the following refined parameters: a = 18.7686(6) Å, b = 15.2482(5) Å, c = 6.90544(25) Å, β = 89.7367(22)°, V = 1976.23(18) Å^3.

The Connolly surfaces[8] for the voids surrounding the two TCE sites in the structure were calculated in the Mercury 3.3.1 program using a probe size of 1.2 Å and a grid spacing of 0.3 Å.

Powder XRD data were also recorded at low temperature (250, 200, 150, 100 and 90 K) on beamline I11 at Diamond Light Source to investigate the effects of temperature on the crystal

structure. No significant changes are observed within the temperature range investigated (except for slight peak shifts due to unit cell contraction), indicating that no solid-state phase transition occurs at low temperature and suggesting that there is no significant change in the extent of disorder in the space averaged/time averaged crystal structure. Clearly, the latter conclusion subsumes the possibility that the dynamic disorder of one TCE molecule at ambient temperature may become static disorder at sufficiently low temperature.
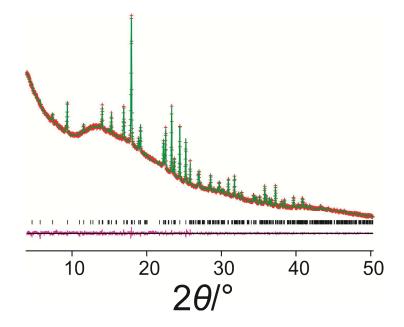

Figure S5   Le Bail fit of the powder XRD pattern of P[5]Q·2TCE for space group P2$_1$ (red + marks, experimental data; green line, calculated data; purple line, difference plot; black tick marks, predicted peak positions).
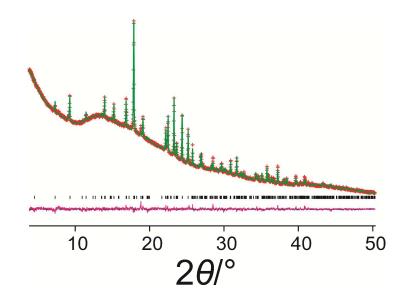

Figure S6   Final Rietveld refinement for P[5]Q·2TCE.

High-Resolution Solid-State ^{13}C NMR of P[5]Q·2TCE

High-resolution solid-state ^{13}C NMR spectra (Figure S7) of P[5]Q·2TCE were recorded at ambient temperature on a Varian VNMRS spectrometer operating at ^{13}C Larmor frequency 100.562 MHz with magic angle spinning at 8 kHz. Spectra were recorded both using the standard ^{1}H→^{13}C CPMAS pulse sequence and using the ^{1}H→^{13}C CPMAS pulse sequence with a dipolar dephasing delay of 50 μs between the CP contact period and spectral acquisition (with no ^{1}H decoupling applied during the dipolar dephasing delay). In spectra recorded with the dipolar dephasing pulse sequence, signals due to _static_ ^{13}C nuclei bonded to at least one ^{1}H nucleus are suppressed; thus, the spectrum only contains signals from _dynamic_ ^{13}C nuclei bonded to at least one ^{1}H nucleus and from ^{13}C nuclei that are not directly bonded to ^{1}H. The dipolar dephasing spectrum for P[5]Q·2TCE contains ^{13}C signals for one TCE molecule, but the ^{13}C signals for the other TCE molecule are suppressed, leading to the conclusion that one TCE molecule undergoes rapid dynamics whereas the other TCE molecule is static. This conclusion is fully consistent with the crystal structure determined from powder XRD data, in which one TCE molecule in the asymmetric unit exhibits disorder (ascribed from the NMR data as dynamic disorder) whereas the other TCE molecule has a single well-defined position, orientation and conformation in the crystal structure.
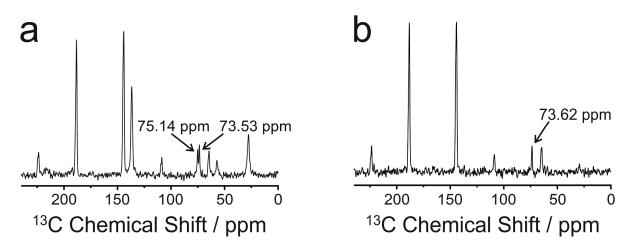

Figure S7   High-resolution solid-state ^{13}C NMR spectra recorded for P[5]Q·2TCE (a) without a dephasing delay and (b) with a dephasing delay of 50 μs. The isotropic peaks at 75.14 ppm and 73.53 ppm in (a) are assigned to the carbon atoms of TCE and are consistent with the assignment that there are two different TCE environments in the crystal structure. In the spectrum recorded with a dephasing delay in (b), the peak at 75.14 ppm is missing, but the peak at 73.62 ppm remains. On this basis, the peak at 75.14 ppm can be assigned as a static TCE molecule and the peak at 73.53 ppm can be assigned as a dynamic TCE molecule.

References

1. Visser, J. W. *J. Appl. Cryst.* **1969**, *2*, 89.
2. Shirley, R. *The CRYSFIRE System for Automatic Powder Indexing: User's Manual*, **1999**, The Lattice Press, Guildford, U.K.
3. Le Bail, A.; Duroy, H.; Fourquet, J. L. *Mat. Res. Bull.* **1988**, *23*, 447.
4. See ref. 21 of paper
5. See ref. 18 of paper
6. See ref. 19 of paper
7. See ref. 20 of paper
8. See ref. 23 of paper